Comparison of Homodyne and Intradyne Detection for High-Order Modulation Schemes in Optical Intersatellite Communication Systems

Semjon Schaefer, Werner Rosenkranz
Chair for Communications
University of Kiel
Kaiserstr. 2, D-24143 Kiel, Germany
sesc@tf.uni-kiel.de

Mark Gregory
TESAT Spacecom
Gerberstraße 49, D-71522 Backnang, Germany
Mark.Gregory@tesat.de

***Abstract*—In order to increase the data rate and lower the power consumption in satellite communication systems, optical laser terminals are an attractive alternative to the conventional RF systems. By using optical coherent detection, high receiver sensitivity as well as full signal recovery is achieved. However, the local oscillator at the receiver requires a carrier recovery system. In order to achieve homodyne detection, an optical phase-locked loop can be used. Each optical PLL structure is fixed to a specific modulation format and its complexity increases with modulation order. Therefore, applying an intradyne detection scheme, where the local laser runs un-synchronized and frequency offset and phase noise compensation is done by digital signal processing after the optical front end, seems to be a possible alternative. We present numerical results for both coherent detection schemes and compare them in terms of receiver sensitivity.**

Keywords— Optical phase-locked loop; homodyne detection; intradyne detection; carrier recovery; digital frequency offset compensation; optical intersatellite link;

I. Introduction

The first European commercial systems providing optical intersatellite communication is the upcoming European Data Relay System (EDRS). This network consists of several satellites in different orbits and allows laser links over distances of up to 45.000 km with data rates of up to 1.8 Gb/s [1]. Due to the lower power consumption and higher data rates optical intersatellite links (OISL) offer an attractive alternative to conventional RF-communication and enable real-time earth observations, like faster earthquake or tsunami forecasts, which require high-speed communication links between satellites and between satellites and earth. Furthermore, the narrow laser beam width ensures a better data security and the lower weight leads to lower overall cost. However, the main challenge is the complex alignment of both satellites to achieve line-of-sight (LOS) connections for data transmission. Therefore, in practical systems a pointing, acquisition and tracking (PAT) system is needed [2].

The OISL core technology as provided for EDRS consists of a laser communication terminal (LCT) which allows optical coherent BPSK data transmission on satellites. The homodyne detection structure uses an optical phase-locked loop (OPLL) to adjust the frequency and phase of the local oscillator (LO) to the incoming signal [3]. However, the OPLL hardware complexity increases by increasing the modulation order. Therefore, the use of intradyne detection, where the local laser runs un-synchronized and which is based on software-defined digital frequency offset compensation, seems to be a possible alternative for future OISL systems.

In the following we numerically investigate and compare these two coherent detection schemes within the optical intersatellite channel. The remainder of the paper is structured as follows: Section 2 gives an introduction to the OISL system. In section 3 the OPLL based homodyne detection scheme and in section 4 the intradyne detection scheme are described. Finally in section 5, we compare both schemes.

II. Optical Intersatellite Link

Optical (inter-)satellite communication describes data transmission between satellites using laser sources in the near-infrared spectrum instead of the conventional radio frequency (RF). Fig. 1 illustrates a typical OISL scenario. As part of an earth observation process a satellite in a low-earth orbit (LEO) may accumulate a high amount of data. This data shall be transmitted to a ground station (GS) on earth in real time, e.g. in case of a fast tsunami forecast system. However, the transmission time window of a LEO satellite is too short (several minutes per day) and the RF link data rate is too low (~Mb/s) in order to send all data to GS during one flyover. Hence, real-time data transmission is not possible. Instead, if

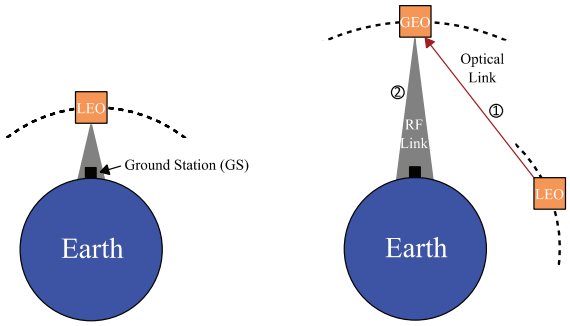

Fig. 1. Conventional RF scenario (left), OISL scenario (right)

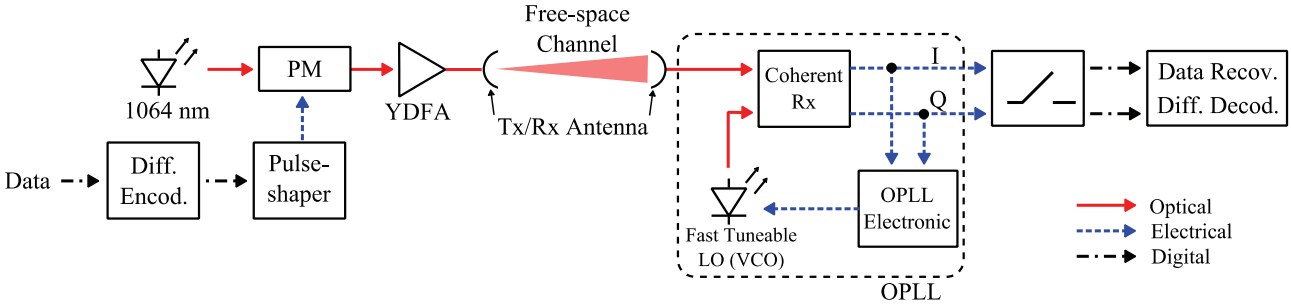

Fig. 2. Homodyne Detection setup of a state-of-the-art optical intersatellite communication system

we assume the data would be available on a satellite in the geostationary orbit (GEO), the time window would be large (24 hours per day). However, the data need to be transmitted fast from the LEO to the GEO satellite. Therefore, an optical link between the satellites with data rates in the range of several Gb/s is used.

Compared to terrestrial optical communication systems, OISL has several differences. First, the equipment has to fulfill different quality requirements. Due to its location in space all parts have to be space-qualified, e.g. in terms of radiation and temperature hardness. Second, the narrow beam width needs line-of-sight between the satellites, so a complex PAT system is needed. Third, once established in space, the system must run for e.g. 15 years in a geostationary orbit without any maintenance. Finally, a significant difference is the in orbit FSO channel, which is less complex than e.g. the optical fiber channel. This is different for FSO transmission through the atmosphere [4].

Fig. 2 illustrates the block diagram of a state-of-the-art OISL-BPSK transmission system with homodyne detection. Usually both, transmitter and receiver part, are implemented in one LCT for each satellite in order to guarantee bidirectional transmission. Due to its high power efficiency, a typical laser source is an optical pumped neodymium-doped yttrium aluminium garnet (Nd:YAG) laser at 1064 nm. The light is externally modulated by a phase-modulator (PM), driven by the electrical data signal and amplified up to 2 W by an ytterbium-doped fiber amplifier (YDFA). After transmission through the free-space channel the received optical signal is detected by the coherent receiver, containing a 90° optical hybrid, which superimposes the receive light with the LO light. Finally, the demodulated signal is sampled and passed to the data recovery. Both lasers, transmitter laser and LO, will show a frequency mismatch, due to the Doppler shift, natural frequency drift and phase noise. In order to ensure homodyne detection this mismatch is eliminated in the optical domain by an OPLL structure. In case of intradyne detection the frequency mismatch will be compensated for in the digital domain by digital signal processing. Both detection schemes will be described in detail in the following sections.

III. OPLL Based Homodyne Detection

The presented OPLL is a Costas-loop based control system as shown in Fig. 3. A 90°-Hybrid transforms the incoming signal $s_1(t)$ into baseband by beating with a local oscillator $s_2(t)$. The LO is controlled by an error signal $x(t)$ or $\varepsilon(t)$ and therefore realized with a fast tuneable Laser. The two signals are described as follows:

$$\begin{aligned} s_1(t) &= \hat{s}_1 \sin\left[\omega_0 t + \phi_1(t) + \phi_M(t)\right] \quad \text{with} \quad \phi_1(t) = \Delta\omega(t)t + \phi_{1,0} \\ s_2(t) &= \hat{s}_2 \cos\left[\omega_0 t + \phi_2(t)\right] \quad \text{with} \quad \phi_2(t) = K_0 \int x(t)dt + \phi_{2,0} \end{aligned} \quad ,(1)$$

where $\hat{s}_{1,2}$ denote the signal amplitudes, ω_0 the carrier frequency, $\Delta\omega(t)$ the time varying frequency offset due to the Doppler shift, K_0 the frequency gain of the VCO in Hz/V, $\phi_M(t)$ the phase modulation, $\phi_{1,0}$ and $\phi_{2,0}$ a constant phase offset. After converting into the electrical domain by the photodiodes and amplification the I- and Q-signal is given as

$$\begin{aligned} U_I(t) &= G{\cdot}R{\cdot}\hat{s}_1\hat{s}_2 \cos\left(\varphi(t) + \phi_M(t)\right) \\ U_Q(t) &= G{\cdot}R{\cdot}\hat{s}_1\hat{s}_2 \sin\left(\varphi(t) + \phi_M(t)\right) \end{aligned} \quad , \qquad (2)$$

where G denotes the gain of the transimpedance amplifier (TIA), R the responsivity of the photodiodes and $\varphi(t) = \phi_1(t) - \phi_2(t)$ the phase error. To ensure a correct frequency acquisition the control signal of the LO should only contain the phase error information and no data. In case of BPSK transmission, i.e. $\phi_M(t) \in \{0, \pi\}$, we get such a data-free error signal by multiplying U_I and U_Q which results in

$$\begin{aligned} \varepsilon(t) &= U_I(t){\cdot}U_Q(t) \\ &= \left(GR\hat{s}_1\hat{s}_2\right)^2 \cos\left(\varphi(t) + \phi_M(t)\right)\sin\left(\varphi(t) + \phi_M(t)\right) \\ &= \frac{\left(GR\hat{s}_1\hat{s}_2\right)^2}{2}\sin\left(2\varphi(t) + 2\phi_M(t)\right) \\ &= K_\mathrm{D}\sin\left(2\varphi(t)\right). \end{aligned} \qquad (3)$$

where $K_\mathrm{D} = \left(GR\hat{s}_1\hat{s}_2\right)^2/2$ denotes the phase discriminator gain. Since K_D directly influences the OPLL behavior it should be kept constant. However, $\hat{s}_2$ continuously change during transmission as the distance between the satellites will vary. Therefore, an automatic gain control (AGC) is used in addition.

The error signal $\varepsilon(t)$ contains the residual frequency offset. It is passed to the loop filter $F(s)$, which describes the control element of the loop and defines the loop dynamic. A typically

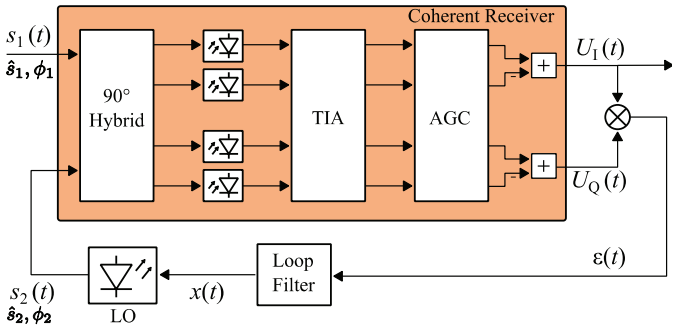

Fig. 3. Optical phase-locked loop based on Costas-loop implementation

used loop filter is the lead-integrator (active) filter with the following transfer function:

$$F(s) = \frac{1 + sT_1}{sT_2}, \tag{4}$$

where the time constants T_1 and T_2 influence the loop dynamic. Finally, the control signal $x(t)$ adjusts the frequency of the fast tuneable LO based on the information of the error signal. Fig. 4 shows a typical frequency lock-in process in an optical intersatellite link with active loop filter observed at the phase error signal $\varepsilon(t)$ and the frequency error (with K_0=5.2 MHz/V, K_D=0.79 V, T_1=0.21 µs, T_2=1.2 µs). The frequency offset between the incoming signal and the LO at the beginning of the lock-in process was set to 5 MHz. In this example the OPLL locks after ~8 µs. Both signals are overlapped by noise. The signals get mainly distorted by two noise sources, phase and shot noise. As typical in optical coherent detection systems the laser phase noise is one of the main signal impairments. Due to their specific linewidth $\Delta\nu$ both, the transmitter laser as well as the local oscillator, cause phase rotation which influences the signal quality. Shot noise is induced in the photodiode caused by stochastic arrivals of photons, which can be modelled as additive Gaussian noise.

In order to further increase the data rate higher-order modulation formats can be used. Besides the well-known modification needed at transmitter side the OPLL has to be modified as well if changing from BPSK to QPSK. In fact the phase discriminator has to be changed, in order to get a data free error signal. As the multiplier operation for BPSK eliminates the data, a possible phase discriminator for QPSK is shown in Fig. 5. The error signal based on that discriminator

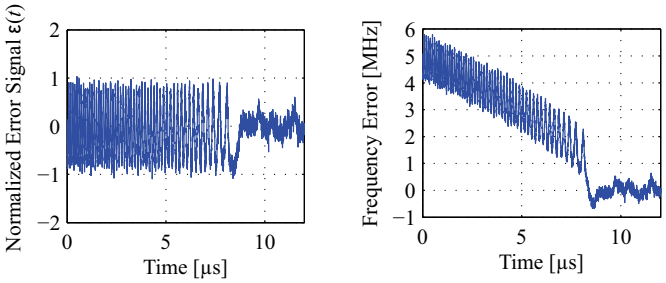

Fig. 4. Lock-in process: phase error (left) and frequency error (right)

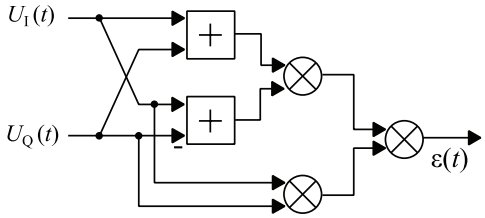

Fig. 5. QPSK phase discriminator

results in

$$\begin{aligned}\varepsilon(t) &= \left[\left(U_I + U_Q\right)\left(U_I - U_Q\right)\right]\left(U_I \cdot U_Q\right) \\ &= K_D \sin(4\phi), \quad \text{with } K_D = \frac{\left(GR\hat{s}_1\hat{s}_2\right)^4}{4}.\end{aligned} \tag{5}$$

Compared to BPSK the error signal for QPSK transmission has a two times higher phase error sensitivity. Therefore, as the OPLL has a sinusoidal nonlinear characteristic the phase error variance has to be further reduced in order to achieve linear behaviour.

Additionally, the system complexity increases when changing from BPSK to QPSK. It would be even more when applying 8-PSK. Therefore, in the following we present an approach for intradyne detection which does not require any analog carrier recovery system and hence reduces hardware complexity.

IV. DSP Based Intradyne Detection

In order to shift the hardware complexity into the digital domain we apply intradyne detection with digital frequency offset compensation. The receiver structure, depicted in Fig. 6, keeps partly the same compared to Fig. 1, except the free-running LO, the obsolete AGC and the now required analog-to-digital converter (ADC) as well as a digital signal processor (DSP). The investigated compensation scheme is separated into coarse (CC) and fine compensation (FC). In the first step, coarse frequency offset compensation is applied, in this case by the phase differential algorithm (PDA) [5, 6]. The sampled input signal to the DSP is assumed to be

$$\begin{aligned}X[k] &= I[k] + jQ[k] \\ &= \hat{A}e^{j\left(\Delta\Phi[k] + \phi_M[k] + \phi_0 + \phi_n[k]\right)} + n[k],\end{aligned} \tag{6}$$

where $\hat{A}$ denotes the intensity of the coherently detected signal, $\Delta\Phi$ the phase shift due to the frequency offset Δf, ϕ_M

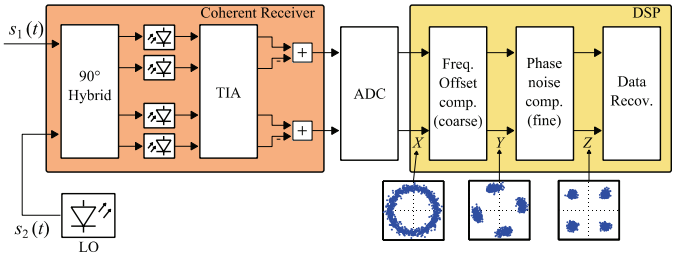

Fig. 6. Intradyne detection based on QPSK-DSP

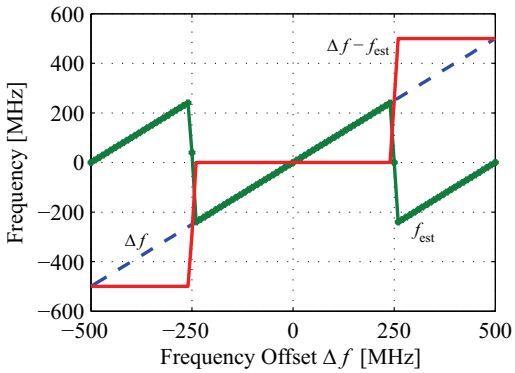

Fig.7. Noise-free behaviour of the digital frequency offset compensation

the data modulation, ϕ_0 a constant phase offset, ϕ_n the phase noise and $n[k]$ the (complex) additive noise. The estimated phase shift $\tilde{\Phi}_{CC}$ due to the frequency offset is computed based on the mean phase difference of L consecutive samples by

$$\tilde{\Phi}_{CC} = \frac{1}{M} \cdot \arg\left\{ \sum_{k=1}^{L} \left(X[k] \cdot X^*[k-1] \right)^M \right\}, \qquad (7)$$

where M denotes the modulation order for M-PSK, i.e. $M = 4$ in case of QPSK, and L is the length of averaging. After re-rotating the incoming samples the output of the coarse compensation stage is

$$Y[k] = X[k] \cdot \exp\left(-j\tilde{\Phi}_{CC}\right). \qquad (8)$$

The final estimated frequency offset is then calculated by

$$f_{est} = \frac{\tilde{\Phi}_{CC}}{2\pi T_s}. \qquad (9)$$

In practical systems, the information about the estimated frequency offset could be used to adjust the local oscillator on the receiver satellite in order to keep the frequency mismatch within a limited range.

Fig. 7 shows the principle of the coarse compensation in case of noise-free BPSK transmission (M=2) and $f_s = 1/\mathrm{T_S} = 1\,\mathrm{GHz}$. Obviously, the algorithm works properly but only in a limited range, here between $\pm 250\,\mathrm{MHz}$. This is due to the fact that the arg{}-operation in (4) wraps the phase if crossing the $\pm\pi$ border. The maximum frequency offset which will be properly estimated is therefore

$$f_{est,\max} = \frac{\pm\pi}{2\pi T_s M} = \frac{\pm 1}{2MT_s}, \qquad (10)$$

which conforms to the result in Fig. 7. If considering noise, the residual frequency error after CC may still reach several MHz. Hence, in a second step, fine compensation based on Viterbi & Viterbi algorithm will reduce the residual frequency offset and phase noise. The incoming data is separated into

TABLE I. SIMULATION PARAMETERS

Tx power	P_{Tx}	32 dBm
Symbol rate	f_s	1 GS/s
Rx bandwidth	B_e	2 GHz
OPLL bandwidth	B_L	350 kHz
FC sample length	N	32
CC sample length	L	1024
Residual FO (intradyne)	Δf	100 MHz
LO power	P_{LO}	12 dBm
Linewidth (Tx/Rx)	$\Delta\nu$	10 kHz

blocks of length N and the mean phase shift of each block i is computed by

$$\tilde{\Phi}_{FC,i} = \frac{1}{M} \arg\left\{ \sum_{n=1}^{N} \left(Y[n + (i-1)N] \right)^M \right\}, \qquad (11)$$

where N denotes the length of averaging.

The resulting output of the fine compensation stage is given by

$$Z[k] = Y[k] \cdot \exp\left(-j\tilde{\Phi}_{FC}\right). \qquad (12)$$

The value of N and L influences the compensation accuracy [6] as well as the computational effort. Therefore, a trade-off between accuracy and effort is required, which depends on the available space-qualified DSP, signal-to-noise ratio (SNR) and initial frequency offset.

Finally, it should be mentioned that software-based frequency compensation additionally allows real-time adaption to different modulation formats, compensation of other impairments like imbalance between I and Q in the IQ-modulator as well as the usage of equalization schemes if required.

V. COMPARISON

Both detection schemes are numerically investigated in a QPSK OISL transmission system based on Fig. 8. The system parameters are given in Table 1. A 2^{16} bit long two-dimensional pseudo random De-Bruijn sequence (PRBS) was mapped to QPSK symbols. As in the real LCT we assume that in a first step the initial Doppler-shift of several GHz was adjusted in real-time by using known trajectory data of the satellite and thermal frequency sweeping. However, a residual frequency offset Δf may remain which will be compensated in the second step either by an OPLL or DSP. In case of homodyne detection and OPLL techniques, we have to distinguish between frequency acquisition and data transmission. Since measuring the bit error ratio (BER) is only possible *after* frequency acquisition was done, we assume perfect acquisition (except phase noise) for simulating the OPLL data demodulation performance. In case of intradyne detection with digital frequency offset compensation the residual frequency offset Δf was set to 100 MHz. Due to the combination of low receive power and high LO-power the

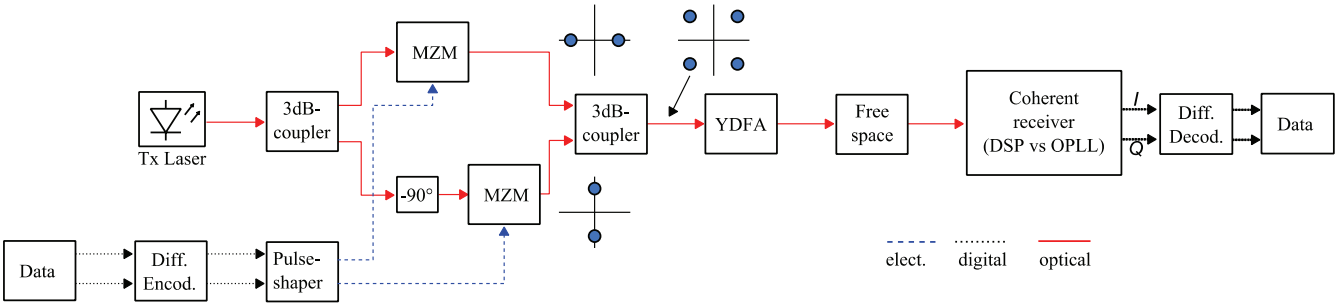

Fig. 8. Block diagram of the QPSK simulation setup

main noise sources are shot and thermal noise at the receiver. Furthermore, phase noise due to the linewidth of Tx and LO laser is considered. Fig. 9 presents the performance evaluation of the two described detection schemes. The BER was determined by Monte-Carlo simulation for BPSK and QPSK, respectively. The received input power was varied by the transmission length. Due to the cycle slip phenomena, i.e. phase jumps of multiple $\pm\frac{2\pi}{M}$ observed at the recovered data symbols, which occur in both receiver schemes, differential (de)-coding was applied in order to avoid burst errors. To achieve error free transmission we aim a BER of 10^{-3}, which allows modern forward error correction codes (FEC) to further decrease the BER.

First of all, both schemes show the expected penalty of 3 dB when changing from BPSK to QPSK for constant symbol rate. The low received input power results from the high free-space attenuation, which requires high receiver sensitivity. Furthermore, the intradyne detection shows an approx. 2 dB better sensitivity, compared to the OPLL, if the laser linewidth is 10 kHz, which is a typical linewidth in state-of-the-art OISL systems. In case of ideal homodyne detection ($\Delta\nu = 0$ kHz), both schemes have nearly the same performance. Hence, the linewidth requirement in case of DSP is less stringent compared to the OPLL setup. It should be noticed, that the simulation does not consider additional noise sources like quantization noise which will further impair practical systems. Nevertheless, this investigation shows the potential of DSP in future OISL systems. Furthermore, in order to keep the OPLL bandwidth in an optimum range, the maximum frequency offset which can be compensated for is much less in case of homodyne detection (some MHz) compared to intradyne detection and the DSP scheme (hundreds of MHz and more). Hence, using an OPLL requires a longer thermal sweeping in order to reduce the initial frequency offset into the working range and the total acquisition time is much longer than for intradyne detection. Since the transmission time window in optical satellite systems is limited by the LOS duration, which will be reduced by the acquisition time, intradyne detection may further extend this time window. However, one essential drawback of intradyne detection is the increased power consumption due to the required DSP.

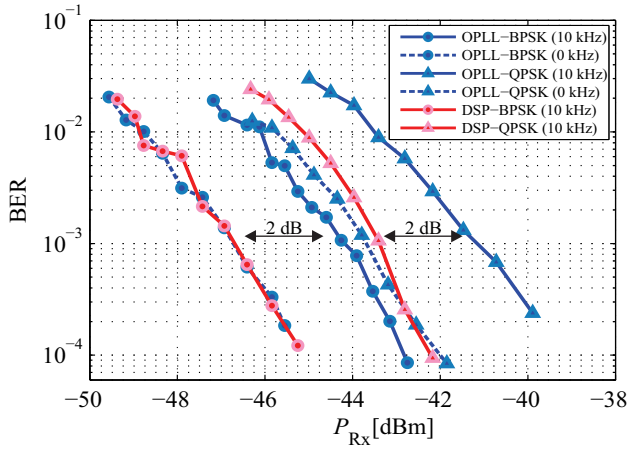

Fig. 9. BER vs. received input power in OISL; comparison of the two detection schemes for BPSK and OPSK

VI. Conclusions

We presented for the first time, to the best of our knowledge, a comparison of homodyne QPSK detection based on OPLL techniques and intradyne detection based on digital frequency offset compensation in optical coherent satellite communication systems. The simulation shows that intradyne detection has nearly the same behaviour as ideal homodyne detection and even improves the receiver sensitivity by approx. 2 dB compared to non-ideal homodyne detection. This indicates the potential of DSP for future OISL systems.

References

[1] Heine, F. et al., "The European Data Relay System, high speed laser based data links," *Advanced Satellite Multimedia Systems Conference and the 13th Signal Processing for Space Communications Workshop (ASMS/SPSC), 2014 7th* , 8-10 Sept., Livorno, 2014

[2] Marshalek. R. et al, in *Near-earth laser communications*, CRC Press, Boca Raton, 2009

[3] Gregory, M. et al., "TESAT laser communication terminal performance results on 5.6 Gbit coherent inter satellite and satellite to ground links," *International Conference on Space Optics*, vol. 4, 2010, p.8, Rhodes, 2010

[4] Gregory, M. et al., "Three years coherent space to ground links: performance results and outlook for the optical ground station equipped with adaptive optics," *Proc. SPIE 8610, Free-Space Laser Communication and Atmospheric Propagation XXV*, 861004, March 19, 2013

[5] Seimetz, M., High-Order Modulation for Optical Fiber Transmission, Springer Ser. in Opt. Sciene,143, Berlin, 2009

[6] Schaefer, S. et al., "Digital Frequency Offset Compensation in High-speed Optical Intersatellite Data Transmission Systems," European Conference on Optical Communications 2015 (ECOC), 27th Sep. – 1st Oct., Valencia, Spain, 2015